Twisted gastrulation enhances BMP signaling through chordin dependent and independent mechanisms

Jing Xie and Shannon Fisher*

The McKusick-Nathans Institute of Genetic Medicine, The Johns Hopkins University School of Medicine, 733 N. Broadway, BRB 455, Baltimore, MD 21205, USA

*Author for correspondence (e-mail: sfisher@jhmi.edu)

Accepted 9 November 2004

Development 132, 383-391
Published by The Company of Biologists 2005
doi:10.1242/dev.01577

Summary

BMP signaling is modulated by a number of extracellular proteins, including the inhibitor Chordin, Tolloid-related enzymes (Tld), and the interacting protein Twisted Gastrulation (Tsg). Although in vitro studies have demonstrated Chordin cleavage by Tld enzymes, its significance as a regulatory mechanism in vivo has not been established in vertebrates. In addition, Tsg has been reported in different contexts to either enhance or inhibit BMP signaling through its interactions with Chordin. We have used the zebrafish gastrula to carry out structure/function studies on Chordin, by making versions of Chordin partially or wholly resistant to Tld cleavage and introducing them into *chordin*-deficient embryos. We examined the cleavage products generated in vivo from wild-type and altered Chordins, and tested their efficacy as BMP inhibitors in the embryo. We demonstrate that Tld cleavage is crucial in restricting Chordin function in vivo, and is carried out by redundant enzymes in the zebrafish gastrula. We also present evidence that partially cleaved Chordin is a stronger BMP inhibitor than the full-length protein, suggesting a positive role for Tld in regulating Chordin. We find that depletion of the embryo for Tsg leads to decreased BMP signaling, and to increased levels of Chordin. Finally, we show that Tsg also enhances BMP signaling in the absence of Chordin, and its depletion can partially rescue the *chordin* mutant phenotype, demonstrating that important components of the BMP signaling pathway remain unidentified.

Key words: Chordin, Twisted gastrulation, BMP, Dorsoventral patterning, Zebrafish

Introduction

Bone morphogenetic protein (BMP) signaling is regulated by complex interactions of inhibitors, proteases and other proteins (Balemans and Van Hul, 2002). The BMP inhibitor Chordin was first identified in *Xenopus* as a factor capable of rescuing axis formation in ultraviolet treated embryos (Sasai et al., 1994), and was subsequently shown to bind BMPs and prevent them from activating their receptors (Piccolo et al., 1996). Many components of the BMP signaling pathway are functionally conserved in *Drosophila*, including *short gastrulation* (*sog*), a homolog of Chordin, and *decapentaplegic* (*dpp*), a homolog of a subset of the vertebrate BMPs (Francois and Bier, 1995; Holley et al., 1995; Schmidt et al., 1995).

Chordin contains four cysteine-rich (CR) domains, similar to those found in a number of extracellular matrix proteins (Sasai et al., 1994). High-affinity binding of Chordin for BMPs resides in its CR domains (Larraín et al., 2000); CR1 and CR3 have significant binding affinity as individual domains, although approximately one-tenth that of the full-length (FL) protein, and the biological activity of FL Chordin and its fragments roughly parallels their binding affinities. These data predict that cleavage of Chordin into smaller fragments would significantly reduce its biological activity as a BMP inhibitor.

tolloid (*tld*) was first identified as a zygotic *Drosophila* gene required for dorsoventral (DV) patterning, and homologous to vertebrate *Bmp1* (Shimell et al., 1991). Tld cleaves Sog at two sites, presumably explaining its ability to enhance Dpp signaling by decreasing the levels of a Dpp inhibitor (Marques et al., 1997). In addition to Bmp1, several other Tld-related vertebrate enzymes have been identified. Some of these similarly cleave Chordin in vitro (Blader et al., 1997; Piccolo et al., 1997; Scott et al., 1999), and when misexpressed in the embryo can antagonize Chordin function (Goodman et al., 1998; Piccolo et al., 1997).

Direct genetic evidence for the importance of vertebrate Tld proteins in regulating Chordin has been less clear. The zebrafish DV patterning gene *mini-fin* (*mfn*; *tll1* – Zebrafish Information Network) encodes a Tld-related enzyme (Connors et al., 1999), which cleaves Chordin in vitro (Blader et al., 1997). However, *mfn* mutants have no phenotype during gastrulation, when *chordin* expression is highest, and the mutation has not been correlated with abnormalities in Chordin cleavage in vivo. In mouse, the *Bmp1* and *Tll1* genes have each been knocked out (Clark et al., 1999; Suzuki et al., 1996), revealing functions in heart septation, body wall closure and collagen processing. However, none of these roles have been correlated with abnormalities in Chordin cleavage in the single mutant mice. Analysis of cells from single and double mutants has shown redundant function for the two enzymes in cleaving Chordin and other substrates (Pappano et al., 2003). Genetic analysis in vertebrates is clearly complicated by the fact that

multiple enzymes cleave Chordin, and redundancy masks the importance of this regulatory mechanism.

The *Drosophila twisted gastrulation* (*tsg*) gene is required for peak Dpp signaling in the dorsal embryo, and also cooperates with Sog to inhibit Dpp signaling (Mason et al., 1994; Mason et al., 1997). Vertebrate Tsg genes have been reported both to enhance (Oelgeschlager et al., 2000; Zakin and De Robertis, 2004) and inhibit (Blitz et al., 2003; Chang et al., 2001; Ross et al., 2001; Scott et al., 2001) BMP signaling. To reconcile these findings, a model has been proposed in which Tsg acts in two steps, first enhancing the binding of Chordin to BMP, then after cleavage helping to displace the Chordin fragments (Larraín et al., 2001). According to this model, the amount of Tld activity determines the balance between these two counteracting functions. In vitro, Tsg increases cleavage of mouse Chordin at the two identified Tld cleavage sites and at an additional, intermediate site not used in the absence of Tsg (Scott et al., 2001). A similar cleavage of Sog occurs in the *Drosophila* embryo, generating a more potent Dpp inhibitor termed 'Supersog' (Yu et al., 2000). If such a cleavage occurs in vivo for the vertebrate protein, it would ascribe a positive role to both Tld and Tsg in Chordin regulation.

We assessed the role of Tld in regulation of Chordin in the zebrafish gastrula and examined the effect of Tsg on Chordin cleavage and function. Through alterations of conserved residues near the cleavage sites, we created Chordin mutants that retain BMP-inhibitory activity but are resistant to Tld cleavage at one or both sites. RNAs encoding wild-type and cleavage mutant (CM) Chordins were used to rescue zebrafish *chordin/dino* (*din*; *chd* – Zebrafish Information Network) mutant embryos. Prevention of cleavage at either site enhances the ability of Chordin to rescue *din* mutants, confirming the importance of cleavage as a regulatory mechanism. We also provide evidence that the product of the downstream cleavage event is a stronger BMP inhibitor than the FL protein, suggesting a positive role for cleavage in Chordin regulation. We show that Chordin cleavage is extremely rapid in vivo, and that redundant enzymes cleave Chordin in *mfn* mutants. However, we find no evidence of alternative cleavage sites being used in either the wild-type or CM proteins. Furthermore, we show that endogenous Tsg decreases steady state Chordin in the embryo, reducing its effectiveness as a BMP inhibitor. We reassessed the *tsg1* (*tsga* – Zebrafish Information Network) morphant phenotype, both in wild-type and *din* mutant backgrounds; we find that the predominant effect of Tsg in the zebrafish gastrula is to enhance BMP signaling, and that it can also do so independently of Chordin.

Materials and methods

Fish stock maintenance

Fish were cared for using standard methods (Westerfield, 1995). The din^{tt250} and mfn^{tm124a} alleles were maintained through intercrossing of heterozygous or homozygous mutant fish. For all injection experiments, clutches of mutant embryos were obtained by intercrossing $din^{-/-}$ or $din^{-/-}; mfn^{-/-}$ fish.

Site-directed mutagenesis

The QuikChange site-directed mutagenesis kit (Stratagene) was used to introduce mutations into the zebrafish *chordin* coding sequence, starting with a previously described injection construct in the pCS2+ vector (Miller-Bertoglio et al., 1997). The sequence surrounding the upstream cleavage site was altered to TTCT**T**CAAC**A**ACAGA, and surrounding the downstream cleavage site to ATG**T**TGCAGGCG**A**A-CGGG (altered bases are in bold). All constructs were verified by sequencing.

Construction of epitope-tagged chordins

The six-copy Myc tag was excised from the pCS2+MT vector with *Cla*I and *Xba*I and inserted following the wild-type and CM-*chordin* coding sequences. To verify that the tagged RNAs gave rise to full-length, stable proteins, they were subjected to in vitro translation and the resulting proteins detected by western blotting for Myc (data not shown). In initial experiments, similar amounts of tagged and untagged RNAs rescued *din* mutants, showing that the Myc sequences did not adversely affect protein activity or stability (data not shown). Therefore, subsequent rescue experiments were performed with the C-terminal tagged constructs.

To construct N-terminal tagged *chordin* vectors, a linker encoding the first 29 amino acids of Chordin was synthesized and inserted into the *Bam*HI site of pCS2+MT. Then the remainder of the wild-type and CM-*chordin* coding sequences were amplified by PCR and inserted into the *Eco*RI and *Xba*I sites downstream of the Myc tags. Although placement of the Myc tag at the N-terminus does somewhat destabilize the protein, these RNAs also rescue *din* mutants at levels comparable with the untagged RNAs, showing that the proteins are functional.

To construct the vector encoding the N+I fragment containing the mutation of the upstream cleavage site ($N+I_A$), the sequence encoding amino acids 1 to 849 of CM_A was amplified and inserted into the pCS2+MT vector between *Bam*HI and *Cla*I.

As a control for quantification of Myc-tagged Chordins, a construct was made encoding a GFP-Myc fusion protein with the signal peptide of Chordin added at its N terminus. This RNA was co-injected with tagged *chordin* RNAs, and the amount of its product used as an internal standard for quantification.

RNA and morpholino injections and phenotypic scoring of injected embryos

The sequence of *tsg1*-MO1 has been previously described (Ross et al., 2001). The non-overlapping MO5 (CGCCGAACTCTGAGCT-GAGCAGAAC), the four-base mismatch to MO1 (CTCATGTTGAT-GATGAACACCGCAT) and the five-base mismatch to MO5 (CCCC-CAACTCTCAGCTCAGCACAAC) were gifts from M. Mullins.

RNAs for injection were transcribed with the mMessage mMachine Sp6 kit (Ambion) from *Not*I linearized templates. RNAs were quantified by spectrophotometry and the amounts confirmed by agarose gel electrophoresis. For each injection experiment, the RNAs encoding different versions of Chordin were synthesized, purified and quantified in parallel. RNA injections were performed as previously described (Fisher and Halpern, 1999). On the following day, embryos were scored using standard phenotypic indicators of excess or decreased BMP signaling (Hammerschmidt et al., 1996; Mullins et al., 1996). For the rescue experiments, 'ventralized' embryos resembled *din* mutants (small brain and somites, excess blood in ventral tail, multiplicated fin folds), 'rescued' embryos appeared wild-type or mildly dorsalized (Class 1, or partially absent ventral fin fold) and 'dorsalized' embryos were those in Class 2-5 (more severe tail defects or truncations, tail curled on top of yolk, some or all somites expanded to encircle the yolk).

Some morphant embryos were fixed at 80% epiboly or 8 to 12 somite stages, and in situ hybridizations performed as previously described (Miller-Bertoglio et al., 1997), using *bmp4*, *chd*, *evel*, *gsc*, *gata2*, *krox20* (*egr2b* – Zebrafish Information Network) and *myod* as markers indicative of DV patterning.

RNA encoding Tsg1 was transcribed as above and co-injected to rescue the *tsg1* morphant phenotype. The construct containing the *Xenopus tsg1* coding sequence, with the signal peptide replaced with that of ECM protein BM40/SPARC, was a gift from M. O'Connor.

Immunoprecipitation and western blotting

Embryos were collected and homogenized in ice cold extraction buffer [250 mM sucrose, 4 mM EDTA, 100 mM NaCl, 10 mM Tris-HCl (pH 7.6)] with added protease inhibitor cocktail (Roche). After centrifugation, the supernatant was incubated with agarose-coupled 9E10 anti-Myc antibody (Santa Cruz Biotech). The pellet was collected by centrifugation, washed four times with RIPA buffer (PBS, 1%NP-40, 0.5% sodium deoxycholate, 0.1% SDS) and one time with 50 mM Tris (pH 6.8). The pellet was resuspended in electrophoresis sample buffer and analyzed by western blotting. Protein gel electrophoresis and immunoblotting were performed according to standard protocols (Harlow and Lane, 1988; Westerfield, 1995). 9E10 anti-Myc antibody (Santa Cruz Biotech) was used to detect tagged Chordin fragments, and blots were visualized with the ECL Plus kit (Amersham). Some blots were scanned with a Storm Phosphorimager; individual bands were quantified using the local average method.

Results

Sequences surrounding the two Tld cleavage sites in Chordin are conserved in several vertebrate species, including zebrafish (Scott et al., 1999). We altered conserved residues at the two sites, to make them resistant to cleavage (Fig. 1A). RNAs encoding cleavage mutant Chordin with the first, second, or both, sites altered (CM_A, CM_B, and CM_{AB}-*chordin*) were injected to rescue Chordin-deficient *din*$^{-/-}$ embryos (Fig. 1B,C) as described previously (Fisher and Halpern, 1999). In initial experiments, successively lower amounts of each RNA were injected until optimal rescue was achieved. CM_{AB} RNA was ~10-fold more potent than wild-type *chordin* in the rescue assay, demonstrating the importance of Tld cleavage in vivo as a mechanism to limit Chordin activity. We predicted that partial cleavage products of Chordin would have reduced BMP-binding affinity, and therefore the partial cleavage mutants would be intermediate in efficacy between wild-type and CM_{AB}. CM_B was ~3-fold more potent than wild type, fitting this prediction. However, CM_A was more potent than CM_{AB}, a result we have repeated in several independent experiments and with multiple batches of RNA (see also Fig. 3A, Fig. 4A).

One possible explanation for the efficacy of CM_A is that cleavage at the upstream site is prerequisite to downstream cleavage. To follow the processing, we injected *chordin* with Myc epitope tags added to the C terminus into *din*$^{-/-}$ embryos, which were lysed and subjected to immunoprecipitation and western blotting (Fig. 1D, left blot). The mutations introduced to the Tld sites largely prevented cleavage as predicted, and cleavage at the two sites occurred independently. The major product from wild-type Chordin was consistent in size with the predicted C-terminal cleavage product. Quantitation of a similar blot showed that in early gastrulation, 6 hours after injection, 93% of the Myc tag was in the C-terminal fragment (data not shown), demonstrating robust, rapid cleavage activity. By contrast, CM_{AB} gave rise to a single prominent band representing FL protein 20 hours after injection. A small amount of lower molecular weight protein could be seen; however, this did not seem to represent cleavage at the normal site, as it appears as a smear rather than a sharp band on longer exposure (data not shown). The C-terminal fragment was the predominant product from CM_A, showing that cleavage at the downstream site is unaffected by mutation of the upstream site. Similarly, from CM_B the major band was slightly smaller than FL protein, produced by cleavage at the upstream site. Interestingly, following injection of the same amounts of

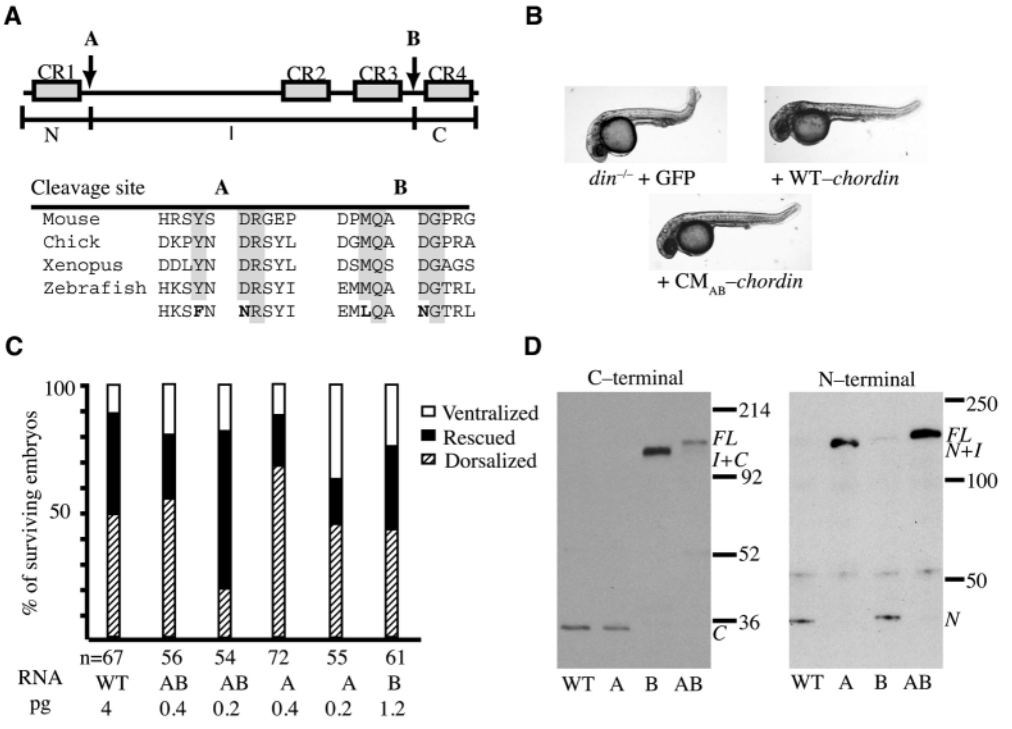

Fig. 1. Tld cleavage regulates Chordin function in vivo. (A) Diagram of Chordin with position of cleavage sites and CR domains indicated. Below are sequences surrounding the Tld cleavage sites in several species, with conserved residues shaded in gray; on the bottom line are the changes introduced by mutagenesis (bold). (B) Embryos were injected with indicated RNAs and sorted the next day; all embryos injected with GFP RNA were ventralized, and indistinguishable from *din* mutants. Approximately 4 pg of *chordin* RNA was required to rescue embryos to wild-type appearance, whereas only 0.4 pg of CM_{AB} RNA was capable of rescue. (C) CM_{AB} was ~10-fold more potent than wild type in the rescue assay. CM_A was ~20-fold more potent, whereas CM_B was only threefold better than wild type. The number of embryos for each RNA amount is indicated under the bar. (D) *din*$^{-/-}$ embryos were each injected with 20 pg of indicated tagged RNAs and subjected to immunoprecipitation and western blotting with anti-Myc at 20 hours (C-terminal) or 5 hours (N-terminal) after injection. The 50 kDa band in the second blot, also seen in Fig. 3B, is present in negative control samples with no injected RNA. The position of molecular weight markers (kDa) and of bands corresponding to predicted cleavage products are indicated to the right of the blots.

RNA, more protein accumulated from CM_B than from the other constructs, a result observed consistently in multiple experiments (see also Fig. 2A). This suggests that a sequence near the N terminus, removed by cleavage at the upstream site, destabilizes Chordin protein.

Although studies on mouse Chordin showed cleavage at an alternative site in the presence of Tsg (Scott et al., 2001), our examination of the C-terminal cleavage products failed to reveal any novel fragments. However, alternative cleavage might be evident only by examination of N-terminal fragments. Therefore, we constructed *chordin* RNAs with Myc epitope tags added to the N terminus, immediately following the signal peptide. When these RNAs were injected into *din* mutants, the major fragments corresponded to predicted cleavage products (Fig. 1D, right blot); the band at ~50 kDa is non-specific and also observed in negative control samples not injected with Myc-tagged RNA. In conclusion, we see no evidence of alternative cleavage products by examining proteins labeled at either the C or N terminus, even when cleavage is prevented at both of the normal Tld sites.

Because of the enhanced accumulation of labeled protein from CM_B, we wanted to also compare the stability of the N-terminal fragments. They generally appeared less stable than C-terminal fragments, but we directly tested the effect of Myc tag position on stability. We injected two groups of embryos with the same amount of CM_{AB} RNA, labeled at either the C or N terminus, and processed the samples in parallel. Similar amounts of labeled proteins were detected 5 hours after injection, but substantially less N-terminal labeled protein at 20 hours (data not shown). Therefore, we could not compare the stability of FL Chordin and the cleavage products over longer periods. However, over shorter time periods, there did not appear to be greater accumulation of labeled protein from CM_A than from CM_{AB} (Fig. 1D and data not shown).

We examined the products of Chordin cleavage at several time points after injection. For wild-type Chordin, almost all detectable protein was in the form of the small C-terminal fragment 8 hours after injection (Fig. 2A). On longer exposure, small amounts of FL protein and I+C fragment were seen, and the amounts decreased slightly from 8-14 hours. For CM_A a similar amount of FL protein was detected at the time points examined (Fig. 2A). For CM_B, significantly more total Myc tag was detected at all time points, as noted above (Fig. 2A). Although in the blot in Fig. 2A it is impossible to resolve the faint band representing FL protein in the CM_B samples, upon longer electrophoresis of additional samples, we verified that a similar amount of FL protein is present in embryos injected with CM_B, CM_A or wild-type *chordin* at 6 hours (Fig. 2C). Over the period examined, we did not observe large differences in cleavage kinetics for the different forms of Chordin, but because of the rapidity of cleavage, we cannot exclude subtle differences.

Our results demonstrate robust endogenous Tld activity in the zebrafish embryo, even prior to gastrulation. The zebrafish DV patterning gene *mfn* encodes a Tld-related enzyme (Connors et al., 1999), shown to cleave Chordin in vitro (Blader et al., 1997). When wild-type *chordin* RNA was injected into *mfn;din* double mutants, an increase in the amount of FL protein was seen (Fig. 2B). However, the majority (>75%) of detectable Myc tag was still on the small C-terminal fragment, showing that redundant enzyme activity

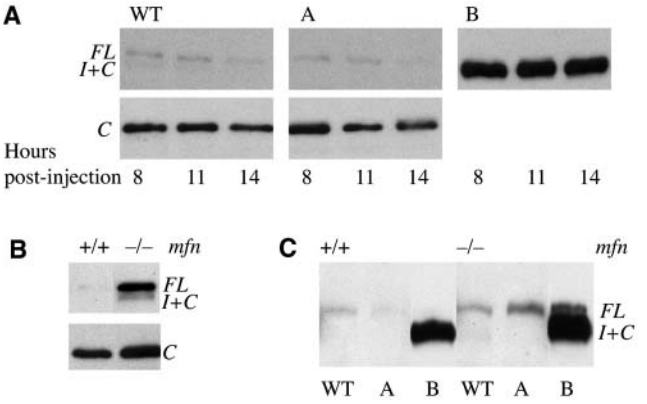

Fig. 2. Chordin is cleaved rapidly by redundant enzymes in zebrafish embryos. (A) $din^{-/-}$ embryos were injected with indicated RNAs and analyzed at varying times after injection. FL protein was not detectable in shorter blot exposures (lower panels); the insets above the gels for wild type and CM_A show a longer exposure. The amounts of FL protein and C-terminal fragment are similar for wild type and CM at the times examined. The I+C fragment from CM_B accumulates at higher levels at all time points. Exposure times were 1 minute for lower panels and CM_B and 20 minutes for upper panels. (B) Wild type *chordin* RNA (20 pg) was injected into $din^{-/-}$ (first lane in each panel) or $mfn^{-/-}$; $din^{-/-}$ (second lane) embryos, and samples processed 20 hours after injection. The major band in both samples corresponds to the small C-terminal fragment (bottom panel). On longer exposure, an increase in FL protein and I+C fragment is seen in the absence of *mfn* (top panel). (C) Reduced cleavage was also observed in *mfn* mutants 6-7 hours after injection, and for CM_A and CM_B. Each embryo received 20 pg of RNA and 120 embryos were analyzed for each sample.

compensates for loss of *mfn*. We also observed slight increases in FL protein for both of the partial CM Chordins (Fig. 2C), indicating that Mfn does not show a strong preference for cleavage either site.

Our rescue data suggest that the N+I fragment of Chordin is a stronger BMP inhibitor than the FL protein. To test this directly, we constructed a version of *chordin* encoding the N+I fragment containing the mutations of the upstream cleavage site in CM_A ($N+I_A$). We compared its efficacy in the rescue of *din* mutants to CM_A and CM_{AB}-Chordin. The $N+I_A$ fragment was slightly more effective than CM_A (Fig. 3A), and both were more effective than CM_{AB}. These CM constructs are useful for separating the effects of cleavage and binding, although they admittedly give rise to stable fragments not present endogenously. However, the N+I fragment is normally produced in the embryo from wild-type Chordin, and is present at steady-state levels comparable with the FL protein (Fig. 3B), suggesting that it could significantly contribute to BMP inhibition in the embryo.

It is possible that an additional protein participates in the binding and preferentially increases the affinity of the N+I fragment for BMPs. Although Tsg displaces the N+I fragment from BMP in vitro (Larraín et al., 2001), it has been shown to enhance the binding of other Chordin fragments and the FL protein (Chang et al., 2001; Larraín et al., 2001; Oelgeschlager et al., 2000; Ross et al., 2001; Scott et al., 2001). To test Tsg as a candidate for this additional protein, we depleted embryos of Tsg function using a previously described antisense

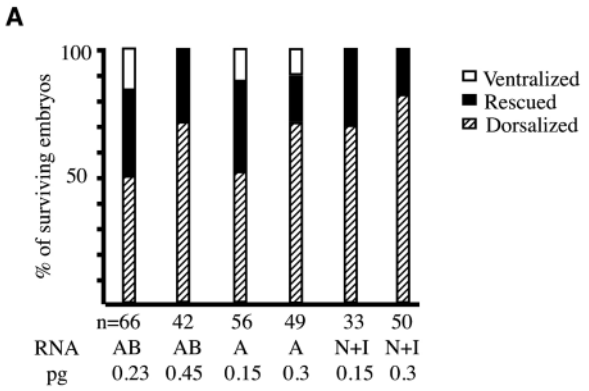

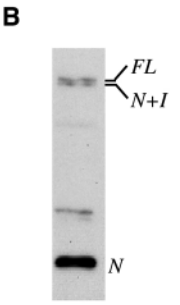

Fig. 3. C-terminally truncated Chordin is a more effective BMP inhibitor. (A) *din*$^{-/-}$ embryos were injected with indicated amounts of RNAs, and sorted the following day for phenotype. Below each bar is the number of embryos. As the N+I fragment is 0.9 times the molecular weight of the FL protein, the same amount of N+I RNA is 1.1 times the moles of the FL RNA. (B) N-terminally tagged wild-type *chordin* RNA was injected at 20 pg per embryo; the Myc label is visualized 5 hours after injection. The N+I fragment is present at comparable levels to the FL protein, although both are present at lower steady-state levels than the short N-terminal fragment.

morpholino directed against *tsg1* (*tsg1*-MO1) (Ross et al., 2001). We rescued *din* mutants with each *chordin* RNA in the absence or presence of *tsg1*-MO1; in every case, the depletion of Tsg resulted in a greater percentage of rescued or dorsalized embryos (Fig. 4A). These data argue that Tsg does not preferentially enhance the binding of the N+I fragment, and further support a general role for Tsg in decreasing the effectiveness of Chordin as a BMP inhibitor.

To determine the mechanism of this effect, we compared the Chordin cleavage products in the absence and presence of *tsg1*-MO1 (Fig. 4B). These experiments were first performed in *mfn;din* double mutants, to enhance the accumulation of FL protein and more readily reveal alterations in the ratio of cleavage products. For all versions of Chordin, more total protein was observed in the presence of *tsg1*-MO1, indicating that endogenous Tsg decreases Chordin levels (Fig. 4C). The

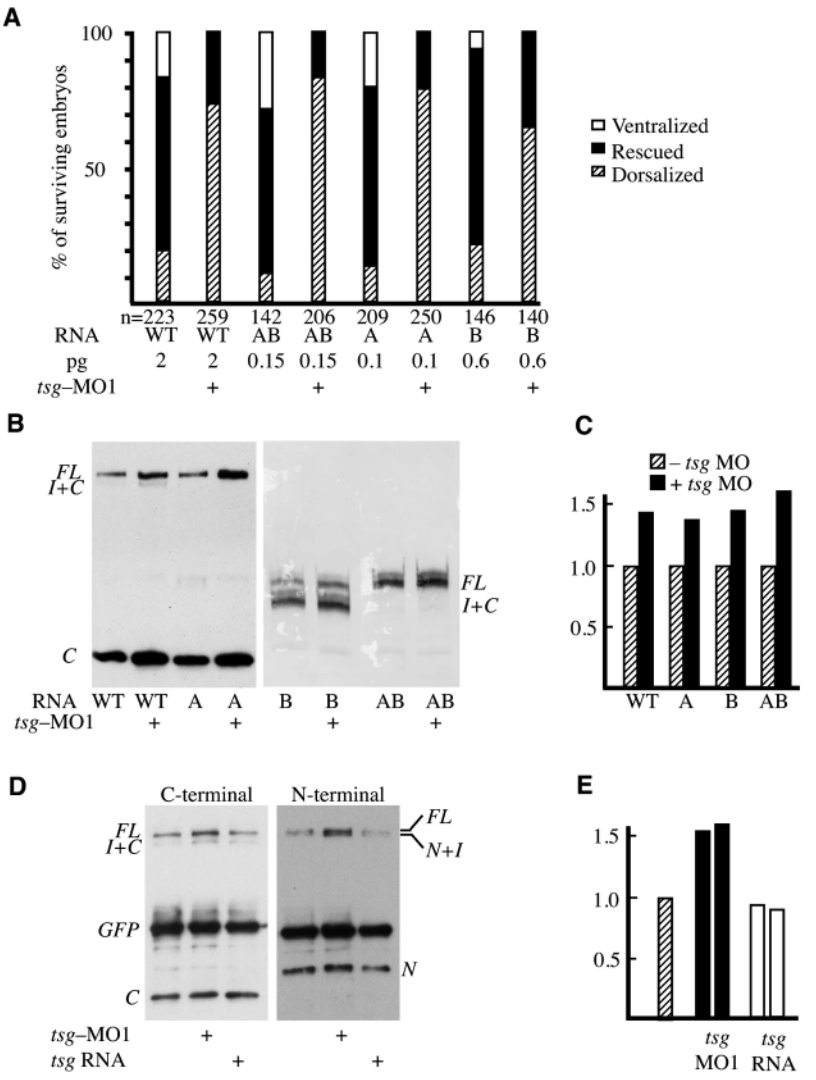

Fig. 4. Tsg decreases steady-state Chordin levels. (A) *din*$^{-/-}$ embryos were injected with indicated amounts of RNAs, in the absence or presence of 6 ng *tsg1*-MO1, and sorted the following day for phenotype. Below each bar is the number of embryos. (B) *din*$^{-/-}$*; mfn*$^{-/-}$ embryos were injected with 20 pg of C-terminally tagged RNAs, in the absence or presence of 15 ng *tsg1*-MO1, and samples processed 5 hours afterwards. The CM_B and CM_{AB} samples were electrophoresed separately to resolve the FL and I+C bands in the CM_B samples. The positions of the major bands are indicated to the left of the first panel, and to the right of the second panel. (C) The blots in B were quantified by phosphorimager, and the sum of all Chordin bands in each lane normalized to numbers of embryos per sample. For the bar graph, the amount of total Chordin in the absence of *tsg1*-MO1 was set to 1.0. (D) *din*$^{-/-}$ embryos were injected as above, with either C-terminally or N-terminally tagged wild-type *chordin* RNA plus Myc-tagged GFP RNA. Injections were also performed, as indicated under the blots, with the addition of *tsg1*-MO1 or 20 pg *tsg1* RNA. (E) The blots in D were quantified, and the sum of all Chordin bands in each sample normalized to the amount of GFP. As above, the amount of Chordin in the absence of *tsg1*-MO or RNA was set to 1.0. In each pair, the left bar indicates level of C-terminally tagged Chordin, and the right bar N-terminally tagged.

ratio of FL protein to cleavage products seen in the wild-type, CM_A and CM_B samples was also slightly greater (6-10%) in the presence of *tsg1*-MO1. This is consistent with previous reports that Tsg enhances Tld cleavage rates (Larraín et al., 2001; Scott et al., 2001; Shimmi and O'Connor, 2003), and further suggests that Tsg does not have a differential effect on cleavage at the two sites. We performed additional experiments in *din* mutants, to verify the effect of Tsg in the presence of Mfn, and also to examine N-terminal fragments. These experiments were performed with the addition of a control RNA encoding Myc-tagged GFP. When the amount of GFP was used as an internal standard to normalize Chordin, we observed similar increases in total Chordin in the presence of *tsg1*-MO1 (Fig. 4D,E). Experiments performed with a control morpholino showed no increase in Chordin (data not shown). We also did not observe products of cleavage at any site between the A and B sites, even when cleavage was prevented at those sites. When wild-type *chordin* was co-injected with *tsg1* RNA to increase Tsg activity, we still observed no additional fragments, nor did we see a large decrease in total Chordin (Fig. 4D,E). This suggests that our failure to observe alternative cleavage was not due to insufficient Tsg.

Our data are inconsistent with previous reports that depletion of Tsg promotes BMP signaling (Blitz et al., 2003; Chang et al., 2001; Scott et al., 2001) and ventralizes the zebrafish embryo (Ross et al., 2001). To test the possibility that Tsg has different roles that predominate at different protein levels, we re-examined the *tsg1* morphant phenotype, injecting different amounts of *tsg1*-MO1 into wild-type embryos. At a lower MO level, we observed some features suggestive of ventralization in the morphants (Fig. 5B,C,N), including a reduced anterior nervous system and blood

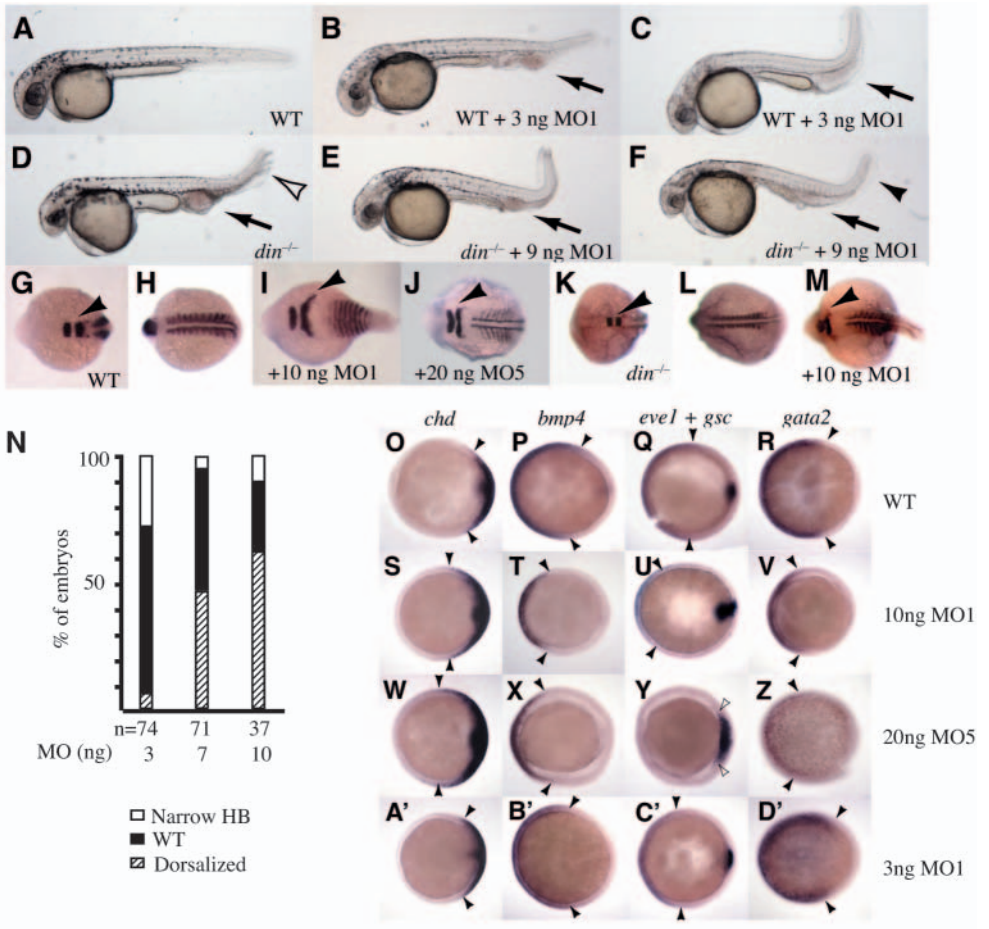

Fig. 5. Tsg enhances BMP signaling and can act independently of Chordin. Wild-type or *din*$^{-/-}$ embryos were injected with the indicated amounts of *tsg1*-MO1, and photographed on the second day following injection (A-F) or fixed and processed for in situ hybridization (G-M). Some wild-type embryos injected with 3-4 ng of *tsg1*-MO1 (B,C) displayed a smaller brain and increased blood in the ventral tail (arrows). However, none displayed multiplication of the ventral fin fold, a prominent feature in ventralized *din* mutants (unfilled arrowhead in D). (E,F) Injection of *tsg1*-MO1 ameliorated some aspects of the *din* mutant phenotype; the excess development of blood was reduced (compare arrows in D-F), and in some embryos the multiplication of the fin fold was corrected (black arrowhead in F). However, anterior nervous system development was not rescued. All embryos in A-F are shown from the side, with anterior towards the left. (G-M) Embryos were injected with the indicated amounts of *tsg1*-MO1 or MO5, fixed at the 8- to 12-somite stage, and processed for in situ hybridization. (I,J) In wild-type embryos, we observed features of dorsalization: lateral expansion of *krox20* expression (arrowhead) and *myod* expression. (L,M) Injection of *tsg1*-MO1 also dorsalized *din*$^{-/-}$ embryos. (N) Wild-type embryos injected with the indicated amounts of *tsg1*-MO1 were fixed and processed for in situ hybridization as above. They were sorted as having a narrowed *krox20* expression domain (Narrow HB); as wild type; or as having a widened expression domain for both markers (Dorsalized). The number of embryos is beneath each bar. (O-D′) Wild-type embryos were injected with indicated amounts of *tsg1*-MOs, fixed at mid-gastrulation (80% epiboly) and processed by in situ hybridization for markers of DV patterning. Expression of *chordin*, a marker for dorsal ectoderm and mesoderm, was expanded in embryos receiving higher amounts of *tsg1*-MOs (S,W), and unchanged in embryos receiving a lower amount of MO1 (A′). By contrast, three different markers of ventral territories (*bmp4*, *eve1* and *gata2*) were decreased (T-V,X,Z) or absent (there is a lack of *eve1* in Y) in embryos receiving high amounts of either MO. In the most strongly dorsalized embryos, *gsc* expression, which marks the dorsal midline tissue, was expanded (unfilled arrowheads in Y). In embryos injected with 3 ng of *tsg1*-MO1, there was increased expression of *gata2*, a marker for ventral ectoderm and hematopoetic cells in the ventral mesoderm (D′); expression of the other markers of ventral territories were unchanged (B′,C′). Embryos in G-M are in dorsal view, with anterior towards the left. (G,H and K,L) Two views of a single embryo rotated to show the *krox20* or *myod* expression. All embryos in O-D′ are shown from the animal pole, with dorsal towards the right; arrowheads indicate the lateral limits of dorsal or ventral markers.

accumulation in the ventral tail. However, the morphants did not have multiplicated ventral fin folds, which is a prominent feature of ventralized *din* and *ogon* mutants (Hammerschmidt et al., 1996). Importantly, at higher MO levels we observed primarily dorsalized phenotypes in the morphants (Fig. 5I,N), consistent with our rescue data and the effect of Tsg depletion on Chordin levels.

To verify our characterization of the morphant phenotypes, we analyzed *tsg1* morphants for markers indicative of DV patterning during gastrulation. We also performed injections with a second, non-overlapping MO targeting the *tsg1* 5′UTR (*tsg1*-MO5). At higher MO levels, we observed consistent expansion of dorsal markers and reduction of ventral markers, indicative of decreased BMP signaling, in embryos injected with either *tsg1*-MO (Fig. 5S-Z). Interestingly, at the lower MO level we did observe a consistent increase in the intensity of *gata2* expression (Fig. 5D′), although it was not accompanied by an increase in expression of other ventral markers or a decrease in expression of dorsal markers (Fig. 5A′-C′). This suggests a specific role for *tsg1* in limiting blood formation downstream of DV patterning, and may account for the increased blood we observe later in embryos injected with a low amount of MO.

As an additional control for the specificity of the morphant phenotypes, we co-injected *tsg1*-MO with *tsg1* RNA (data not shown). At the lower MO level, 1 pg of *tsg1* RNA rescued the phenotype of blood accumulation in the ventral tail, but did not correct the narrowing of the anterior nervous system, supporting our belief that it is non-specific. At the higher MO level, *tsg1* RNA also corrected the features of dorsalization. We also performed injections with mismatch control MOs, and observed none of the phenotypes produced with either high or low amounts of the specific MOs.

Another possible explanation for the disparate roles ascribed to Tsg is that it acts on Chordin to decrease its efficacy as a BMP inhibitor, and simultaneously inhibits BMP signaling through an independent mechanism. To test this hypothesis, we injected *tsg1*-MO1 into *din* mutants. Surprisingly, this depletion of Tsg partially rescued or even dorsalized *din* mutants (Fig. 5E,F,L,M). These results provide strong evidence that Tsg also can act independently of Chordin, but to further enhance rather than inhibit BMP signaling.

Discussion

Assessment of the importance of Chordin cleavage has been complicated in vertebrates by genetic redundancy. Therefore, we used a non-genetic approach, mutating conserved residues at the Tld sites in Chordin to render them resistant to cleavage. The altered Chordins were introduced into Chordin-deficient embryos and their effects on embryonic patterning analyzed. This approach allowed us to test directly the importance of Chordin cleavage, examine the cleavage products under various conditions, and determine the role of Tsg in regulating Chordin cleavage and efficacy in vivo. Although RNA injections are widely used in zebrafish embryos, and often to express mutated gene products, our study combines RNA rescue with structure/function correlations and the biochemical analysis of protein processing. Given the large number of zebrafish mutants with embryonic phenotypes that can be rescued by RNA injection, this general approach should have wide applicability in understanding signaling pathways in early development.

Chordin cleavage is an important regulatory mechanism in the zebrafish gastrula

Previously we have shown that *chordin* RNA injected into embryos at the one-cell stage is detectable by in situ hybridization for ~10 hours (Fisher and Halpern, 1999). Therefore, at 5 hours after injection there is still RNA available for new protein synthesis. However, at this time point the large majority of Chordin has been cleaved, demonstrating robust endogenous Tld activity even prior to gastrulation. Our data further show that cleavage at the A and B sites occurs independently and that the kinetics of cleavage are not significantly different for wild-type and CM Chordins.

The unexpectedly mild phenotype of the zebrafish mutant *mfn* has led to speculation that, at least in zebrafish, Chordin cleavage does not play an important role in DV patterning during gastrulation (Connors et al., 1999; Oelgeschlager et al., 2003; Zakin and De Robertis, 2004). We show instead that redundant enzyme activity compensates for loss of *mfn*. Both during and after gastrulation, the majority of Chordin protein is cleaved in *mfn* mutants, although measurably less than in wild type. In mouse, the Tld-related *Bmp1* and *Tll1* gene products function redundantly to cleave Chordin and other substrates (Pappano et al., 2003). The *mfn* gene is most closely homologous to *Tll1* (Scott et al., 1999); we have identified zebrafish ESTs corresponding to a second ortholog of *Tll1*, which is strongly expressed in the early embryo (J.X. and S.F., unpublished). The product of this gene is a likely candidate for at least some of the Tld activity present in *mfn* mutants.

Positive role for Tld in Chordin regulation

Although mutating either cleavage site increased the efficacy of Chordin as a BMP inhibitor, the effect of alterations at the two sites was not equal. Prevention of cleavage at both sites resulted in a stable FL protein ~10 times more effective as a BMP inhibitor. However, by preventing cleavage at the upstream site, we created a C-terminally truncated Chordin fragment that was even more effective than the stable FL protein. Another protein may participate in Chordin-BMP binding in vivo, selectively increasing the effectiveness of the truncated Chordin. Our data indicate that Tsg is unlikely to play this role, as it decreases the efficacy of all cleavage forms of Chordin. In fact, although there is evidence from a number of in vitro binding studies that Tsg enhances the binding of FL Chordin to BMP (Larraín et al., 2001; Oelgeschlager et al., 2000; Scott et al., 2001), our data indicate that this is not its predominant role in vivo. If it were, then the efficacy of CM_{AB} would decrease in embryos depleted of Tsg.

The N+I fragment may be more stable than the FL protein, as we observed for the I+C fragment. It is difficult to assess this because of the destabilizing effect of N-terminal Myc epitopes. However, at several time points there appeared to be comparable levels of labeled protein accumulated from the CM_A and CM_{AB} constructs (see Fig. 1D; data not shown), making this unlikely. We favor the possibility that CR4, which has little BMP binding affinity or biological activity on its own (Larraín et al., 2000; Scott et al., 2001), actually decreases the overall binding affinity of the FL protein.

There is evidence in *Drosophila* for an alternative cleavage

product of Sog with enhanced Dpp inhibitory activity, whose creation is promoted by Tsg (Yu et al., 2000). Tsg also enhances Chordin cleavage at an intermediate site in vitro, suggesting that a parallel event occurs for the vertebrate proteins (Scott et al., 2001). However, we see no evidence of alternative cleavage products, either when cleavage is prevented at both of the normal Tld sites or when *tsg1* is overexpressed by RNA injection. We cannot rule out that this cleavage event takes place in a small region of the embryo, or in specific tissues later in development. However, the necessary components (Chordin, Tld enzymes, and Tsg) are all present in the gastrula, and we should be able to detect fragments present even at less than 1% of the total label on our western blots. Therefore, we conclude that such cleavage is not likely to play a significant role in the gastrula.

Tld cleavage might also play a positive role if Chordin fragments have novel activities, independent of BMP binding. However, several lines of evidence argue against this. In particular, the epistatis between *dino* and the BMP mutants *swirl* and *snailhouse* has been examined (Wagner and Mullins, 2002). That study confirmed that the BMP mutant phenotypes are epistatic to *dino*, and importantly discovered no additional phenotypes in the double mutants, as would be expected if Chordin or its fragments had functions independent of BMP. We also find that CM_{AB}-Chordin is capable of fully rescuing the *din* phenotype, which would not be the case if the fragments had independent functions.

Tsg decreases steady-state levels of Chordin

To test the effect of Tsg on Chordin efficacy in our system, and the dependence of the effect on cleavage by Tld at either site, we performed rescue experiments with wild-type and CM-*chordin* RNAs in the absence or presence of *tsg1*-MO. In every case, the rescue was more effective under conditions of lowered Tsg, suggesting that Tsg normally acts to suppress Chordin function in the zebrafish embryo. To determine the molecular basis of this effect, we examined Chordin cleavage products resulting from these experiments. The consistent effect of Tsg depletion was to increase steady-state Chordin levels. It has been previously shown that Tsg has the net effect of destabilizing Chordin (Oelgeschlager et al., 2003) and that *Drosophila* Tsg has a similar effect on Sog (Shimmi and O'Connor, 2003), consistent with our data. However, proposed mechanisms for this destabilization have invoked Tld cleavage. We see a similar effect on levels of wild-type and CM_{AB}-chordin in *tsg1* morphants, suggesting that this effect is in part independent of Tld cleavage. We do observe a low level of cleavage or degradation of CM_{AB}-Chordin, although it appears not to represent cleavage at the normal site, it may still be mediated by Tld. To resolve this question definitively would require elimination of all Tld activity from the zebrafish gastrula, a challenge given the genetic redundancy.

Endogenous Tsg enhances BMP signaling through Chordin dependent and independent mechanisms

Contradictory roles have been ascribed to Tsg in modulating vertebrate BMP signaling. However, Tsg has been reported in zebrafish embryos to cooperate with Chordin to inhibit BMPs (Ross et al., 2001). To reconcile our data with these published results, we performed additional Tsg depletions with different levels of *tsg1*-MOs. By injecting lower amounts, we did produce features suggestive of a ventralized phenotype. However, we did not see multiplicated ventral fin folds in any of the morphants, although this is a sensitive indicator of increased BMP signaling and is a consistent feature of the ventralized *din* and *ogon* mutants (Hammerschmidt et al., 1996). We did observe narrowing of the anterior nervous system, but morpholinos can induce non-specific toxic effects in zebrafish (Heasman, 2002), including widespread cell death and neural degeneration (Braat et al., 2001; Lele et al., 2001). In support of this possibility, increased apoptosis occurs in the brains of *tsg1* morphants (Little and Mullins, 2004) and is not seen in ventralized *din* mutants (Fisher et al., 1997). Interestingly, we did observe increased expression of *gata2* in embryos receiving a lower dose of MO. Increased *gata2* expression was also previously reported in *tsg1* morphants, and cited as evidence of their ventralization (Ross et al., 2001). However, the increase is apparently downstream of alterations in DV patterning, and may point to a specific role for *tsg1* in limiting formation of blood or ventral ectoderm. Injection of higher levels of *tsg1*-MOs dorsalized the morphants, which we confirmed by examination of multiple markers during gastrulation. Our results show that endogenous Tsg enhances BMP signaling in vivo, in part by destabilizing Chordin.

Several previous studies of the effects of Tsg in the embryo relied on RNA overexpression. In our hands, *tsg1* RNA dorsalizes both wild-type and $din^{-/-}$ embryos, showing that the effect does not depend on Chordin (data not shown). This result is apparently at odds with our analysis of *tsg1* morphants, and might suggest a normal role for Tsg in inhibiting BMPs. However, Tsg binds BMPs with an affinity comparable with that of individual Chordin CR domains (Chang et al., 2001; Oelgeschlager et al., 2000; Scott et al., 2001). We speculate that, when overexpressed, Tsg can bind BMPs sufficiently to prevent receptor activation, although this does not reflect its normal function. Interestingly, mutated versions of Tsg which do not bind BMPs hyperventralize the zebrafish embryo (Oelgeschlager et al., 2003), consistent with the possibility that the dorsalization seen with overexpression is due to direct BMP binding.

Many proteins in addition to Chordin contain repeated CR domains, and it has been proposed that Tsg could also interact with some of these (Garcia Abreu et al., 2002; Oelgeschlager et al., 2003). We tested the possibility that Tsg decreases the efficacy of Chordin while simultaneously inhibiting BMP signaling through another interaction. However, depletion of Tsg in din mutants ameliorated features of the mutant phenotype and even dorsalized the mutants. Thus, endogenous Tsg enhances BMP signaling both in the presence and absence of Chordin, either through direct interaction with BMPs or in conjunction with other unidentified modulating proteins. Although we cannot rule out that Tsg inhibits BMP signaling under some circumstances, we show that it does not do so in the zebrafish gastrula.

We thank M. Mullins and S. Little for the gift of morpholinos, and for sharing data prior to publication; we thank M. O'Connor for the gift of the tsg1 expression plasmid. This work was funded by the March of Dimes (S.F.).

References

Balemans, W. and van Hul, W. (2002). Extracellular regulation of BMP signaling in vertebrates: a cocktail of modulators. *Dev. Biol.* **250**, 231-250.

Blader, P., Rastegar, S., Fischer, N. and Strahle, U. (1997). Cleavage of the BMP-4 antagonist chordin by zebrafish tolloid. *Science* **278**, 1937-1940.

Blitz, I. L., Cho, K. W. and Chang, C. (2003). Twisted gastrulation loss-of-function analyses support its role as a BMP inhibitor during early Xenopus embryogenesis. *Development* **130**, 4975-4988.

Braat, A. K., van de Water, S., Korving, J. and Zivkovic, D. (2001). A zebrafish vasa morphant abolishes vasa protein but does not affect the establishment of the germline. *Genesis* **30**, 183-185.

Chang, C., Holtzman, D., Chau, S., Chickering, T., Woolf, E., Holmgren, L., Bodorova, J., Gearing, D., Holmes, W. and Brivanlou, A. (2001). Twisted gastrulation can function as a BMP antagonist. *Nature* **410**, 483-487.

Clark, T. G., Conway, S. J., Scott, I. C., Labosky, P. A., Winnier, G., Bundy, J., Hogan, B. L. and Greenspan, D. S. (1999). The mammalian Tolloid-like 1 gene, Tll1, is necessary for normal septation and positioning of the heart. *Development* **126**, 2631-2642.

Connors, S. A., Trout, J., Ekker, M. and Mullins, M. C. (1999). The role of *tolloid/mini fin* in dorsoventral pattern formation of the zebrafish embryo. *Development* **126**, 3119-3130.

Fisher, S. and Halpern, M. E. (1999). Patterning the zebrafish axial skeleton requires early *chordin* function. *Nat. Genet.* **23**, 442-446.

Fisher, S., Amacher, S. L. and Halpern, M. E. (1997). Loss of cerebum function ventralizes the zebrafish embryo. *Development* **124**, 1301-1311.

Francois, V. and Bier, E. (1995). Xenopus chordin and Drosophila short gastrulation genes encode homologous proteins functioning in dorsal-ventral axis formation. *Cell* **80**, 19-20.

Garcia-Abreu, J., Coffinier, C., Larrain, J., Oelgeschlager, M. and de Robertis, E. M. (2002). Chordin-like CR domains and the regulation of evolutionarily conserved extracellular signaling systems. *Gene* **287**, 39-47.

Goodman, S. A., Albano, R., Wardle, F. C., Matthews, G., Tannahill, D. and Dale, L. (1998). BMP1-related metalloproteinases promote the development of ventral mesoderm in early Xenopus embryos. *Dev. Biol.* **195**, 144-157.

Hammerschmidt, M., Pelegri, F., Mullins, M. C., Kane, D. A., van Eeden, F. J., Granato, M., Brand, M., Furutani-Seiki, M., Haffter, P., Heisenberg, C. P. et al. (1996). *dino* and *mercedes*, two genes regulating dorsal development in the zebrafish embryo. *Development* **123**, 95-102.

Harlow, E. and Lane, D. (1988). *Antibodies: A Laboratory Manual.* Cold Spring Harbor, NY: Cold Spring Harbor Laboratory Press.

Heasman, J. (2002). Morpholino oligos: making sense of antisense? *Dev. Biol.* **243**, 209-214.

Holley, S. A., Jackson, P. D., Sasai, Y., Lu, B., de Robertis, E. M., Hoffmann, F. M. and Ferguson, E. L. (1995). A conserved system for dorsal-ventral patterning in insects and vertebrates involving sog and chordin. *Nature* **376**, 249-253.

Larraín, J., Bachiller, D., Lu, B., Agius, E., Piccolo, S. and de Robertis, E. M. (2000). BMP-binding modules in chordin: a model for signalling regulation in the extracellular space. *Development* **127**, 821-830.

Larraín, J., Oelgeschlager, M., Ketpura, N. I., Reversade, B., Zakin, L. and de Robertis, E. M. (2001). Proteolytic cleavage of Chordin as a switch for the dual activities of Twisted gastrulation in BMP signaling. *Development* **128**, 4439-4447.

Lele, Z., Bakkers, J. and Hammerschmidt, M. (2001). Morpholino phenocopies of the swirl, snailhouse, somitabun, minifin, silberblick, and pipetail mutations. *Genesis* **30**, 190-194.

Little, S. C. and Mullins, M. C. (2004). Twisted gastrulation promotes BMP signaling in zebrafish dorsal-ventral axial patterning. *Development* **131**, 5825-5835.

Marques, G., Musacchio, M., Shimell, M. J., Wunnenberg-Stapleton, K., Cho, K. W. and O'Connor, M. B. (1997). Production of a DPP activity gradient in the early Drosophila embryo through the opposing actions of the SOG and TLD proteins. *Cell* **91**, 417-426.

Mason, E. D., Konrad, K. D., Webb, C. D. and Marsh, J. L. (1994). Dorsal midline fate in Drosophila embryos requires twisted gastrulation, a gene encoding a secreted protein related to human connective tissue growth factor. *Genes Dev.* **8**, 1489-1501.

Mason, E. D., Williams, S., Grotendorst, G. R. and Marsh, J. L. (1997). Combinatorial signaling by Twisted Gastrulation and Decapentaplegic. *Mech. Dev.* **64**, 61-75.

Miller-Bertoglio, V., Fisher, S., Sánchez, A., Mullins, M. and Halpern, M. E. (1997). Differential regulation of chordin expression in zebrafish mutants. *Dev. Biol.* **192**, 537-550.

Mullins, M. C., Hammerschmidt, M., Kane, D. A., Odenthal, J., Brand, M., van Eeden, F. J., Furutani-Seiki, M., Granato, M., Haffter, P., Heisenberg, C. P. et al. (1996). Genes establishing dorsoventral pattern formation in the zebrafish embryo: the ventral specifying genes. *Development* **123**, 81-93.

Oelgeschlager, M., Larrain, J., Geissert, D. and de Robertis, E. M. (2000). The evolutionarily conserved BMP-binding protein Twisted gastrulation promotes BMP signalling. *Nature* **405**, 757-763.

Oelgeschlager, M., Reversade, B., Larrain, J., Little, S., Mullins, M. C. and de Robertis, E. M. (2003). The pro-BMP activity of Twisted gastrulation is independent of BMP binding. *Development* **130**, 4047-4056.

Pappano, W. N., Steiglitz, B. M., Scott, I. C., Keene, D. R. and Greenspan, D. S. (2003). Use of Bmp1/Tll1 doubly homozygous null mice and proteomics to identify and validate in vivo substrates of bone morphogenetic protein 1/tolloid-like metalloproteinases. *Mol. Cell. Biol.* **23**, 4428-4438.

Piccolo, S., Sasai, Y., Lu, B. and de Robertis, E. M. (1996). Dorsoventral patterning in Xenopus: inhibition of ventral signals by direct binding of chordin to BMP-4. *Cell* **86**, 589-598.

Piccolo, S., Agius, E., Lu, B., Goodman, S., Dale, L. and de Robertis, E. M. (1997). Cleavage of Chordin by Xolloid metalloprotease suggests a role for proteolytic processing in the regulation of Spemann organizer activity. *Cell* **91**, 407-416.

Ross, J., Shimmi, O., Vilmos, P., Petryk, A., Kim, H., Gaudenz, K., Hermanson, S., Ekker, S., O'Connor, M. and Marsh, J. (2001). Twisted gastrulation is a conserved extracellular BMP antagonist. *Nature* **410**, 479-483.

Sasai, Y., Lu, B., Steinbeisser, H., Geissert, D., Gont, L. K. and de Robertis, E. M. (1994). *Xenopus chordin*: a novel dorsalizing factor activated by organizer-specific homeobox genes. *Cell* **79**, 779-790.

Schmidt, J., Francois, V., Bier, E. and Kimelman, D. (1995). Drosophila short gastrulation induces an ectopic axis in Xenopus: evidence for conserved mechanisms of dorsal-ventral patterning. *Development* **121**, 4319-4328.

Scott, I. C., Blitz, I. L., Pappano, W. N., Imamura, Y., Clark, T. G., Steiglitz, B. M., Thomas, C. L., Maas, S. A., Takahara, K., Cho, K. W. Y. et al. (1999). Mammalian BMP-1/Tolloid-related matalloproteinses, including novel family member mammalian tolloid-like 2, have differential enzymatic activities and distributions of expression relevant to patterning and skeletogenesis. *Dev. Biol.* **213**, 283-300.

Scott, I., Blitz, I., Pappano, W., Maas, S., Cho, K. and Greenspan, D. (2001). Homologues of twisted gastrulation are extracellular cofactors in antagonism of BMP signaling. *Nature* **410**, 475-478.

Shimell, M. J., Ferguson, E. L., Childs, S. R. and O'Connor, M. B. (1991). The *Drosophila* dorsal-ventral patterning gene *tolloid* is related to human bone morphogenetic protein 1. *Cell* **67**, 469-481.

Shimmi, O. and O'Connor, M. B. (2003). Physical properties of Tld, Sog, Tsg and Dpp protein interactions are predicted to help create a sharp boundary in Bmp signals during dorsoventral patterning of the Drosophila embryo. *Development* **130**, 4673-4682.

Suzuki, N., Labosky, P. A., Furuta, Y., Hargett, L., Dunn, R., Fogo, A. B., Takahara, K., Peters, D. M., Greenspan, D. S. and Hogan, B. L. (1996). Failure of ventral body wall closure in mouse embryos lacking a procollagen C-proteinase encoded by *Bmp1*, a mammalian gene related to *Drosophila tolloid*. *Development* **122**, 3587-3595.

Wagner, D. S. and Mullins, M. C. (2002). Modulation of BMP activity in dorsal-ventral pattern formation by the chordin and ogon antagonists. *Dev. Biol.* **245**, 109-123.

Westerfield, M. (1995). *The Zebrafish Book*. Eugene, OR: University of Oregon Press.

Yu, K., Srinivasan, S., Shimmi, O., Biehs, B., Rashika, K. E., Kimelman, D., O'Connor, M. B. and Bier, E. (2000). Processing of the *Drosophila* Sog protein creates a novel BMP inhibitory activity. *Development* **127**, 2143-2154.

Zakin, L. and de Robertis, E. M. (2004). Inactivation of mouse Twisted gastrulation reveals its role in promoting Bmp4 activity during forebrain development. *Development* **131**, 413-424.